REGULAR ARTICLE

blood advances

TNIK as a molecular switch regulating platelet function in hemostasis and hyperlipidemia-associated thrombosis

Li Li,[1,2,*] Xiaoyan Chen,[1,2,*] Jingke Li,[1,2] Xin Deng,[1,2] Yilin Sheng,[1,2] Linrong Lu,[3-5] and Hu Hu[1,2]

[1]Department of Pathology and Pathophysiology and Bone Marrow Transplantation Center of The First Affiliated Hospital, Zhejiang University School of Medicine, Hangzhou, China; [2]Institute of Hematology, Zhejiang University and Zhejiang Engineering Laboratory of Stem Cells and Immunotherapy, Hangzhou, China; [3]Department of Cardiology of The Second Affiliated Hospital, Zhejiang University School of Medicine, Hangzhou, China; [4]Institute of Immunology and Department of Rheumatology, Sir Run Run Shaw Hospital, Zhejiang University School of Medicine, Hangzhou, China; and [5]Shanghai Immune Therapy Institute, Shanghai Jiao Tong University School of Medicine Affiliated Renji Hospital, Shanghai, China

Key Points

- TNIK deficiency in platelets impairs normal hemostasis yet accelerates thrombosis under metabolic stress conditions.
- Platelet TNIK promotes hemostasis via JNK signaling but prevents hyperlipidemic thrombosis by suppressing NOX2/ROS/ERK5 pathways.

Platelets must balance hemostatic function with pathological thrombosis, particularly under metabolic stress conditions. MAPKs are central to platelet responses, but how these platelet signals differentially regulate hemostasis remains poorly understood. To investigate the role of Traf2/Nck-interacting kinase (TNIK), we generated megakaryocyte/platelet-specific TNIK knockout mice (*Tnik*$^{f/f}$ *PF4-Cre*$^{+}$) and evaluated platelet function, hemostasis, and thrombosis under normal and hyperlipidemic conditions using chimeric *Tnik*$^{f/f}$ *PF4-Cre*$^{+}$ *Apoe*$^{-/-}$ mice fed high-fat diets. TNIK-deficient mice exhibited prolonged bleeding times, delayed arterial thrombosis and reduced platelet activation under normal conditions, primarily due to impaired dense granule secretion. Mechanistically, TNIK interacted with c-Jun N-terminal kinase interacting protein 1 to promote mixed lineage kinase 3/mitogen-activated protein kinase kinase 4/c-Jun N-terminal kinase pathway activation during hemostatic responses. Surprisingly, under hyperlipidemic conditions, TNIK deficiency accelerated thrombosis and enhanced platelet responses to oxidized low-density lipoprotein. In this context, TNIK specifically bound to protein kinase C ε and suppressed the NADPH oxidase 2/reactive oxygen species/extracellular signal-regulated kinase 5 pathway, thereby inhibiting excessive platelet activation. We conclude that TNIK functions as a molecular switch in platelets, promoting normal hemostasis while simultaneously preventing hyperlipidemia-associated thrombosis through distinct signaling pathways. This dual regulatory mechanism provides insight into how platelets balance hemostatic function with pathological thrombosis risk and identifies TNIK as a potential therapeutic target in metabolic thrombotic disorders.

Introduction

Platelets serve as critical sentinels of vascular integrity, rapidly responding to vessel injury to prevent bleeding while avoiding inappropriate activation that would cause thrombosis.[1] This delicate balance becomes particularly challenging under metabolic stress conditions such as hyperlipidemia,[2,3] in which platelets face competing signals from both physiological and pathological stimuli. The regulatory

Submitted 11 July 2025; accepted 18 November 2025; prepublished online on *Blood Advances* First Edition 9 January 2026. https://doi.org/10.1182/bloodadvances.2025017737.

*L. Li and X.C. contributed equally to this study.

Original data are available from the corresponding author, Hu (huhu@zju.edu.cn), on request.

The full-text version of this article contains a data supplement.

mechanisms that allow platelets to distinguish between these signals and maintain appropriate responses remain poorly understood, representing a critical knowledge gap in thrombosis research.

MAPKs constitute a central signaling hub in platelets, orchestrating responses to various stimuli.[4] These kinases coordinate essential platelet functions including granule secretion, integrin activation, and thrombus formation. Recent evidence suggests that platelets differentially allocate MAPK signaling under physiological vs pathological conditions. For instance, p38[5,6] and c-Jun N-terminal kinase (JNK)[3,7] participate in both hemostatic processes and oxidized low-density lipoprotein (ox-LDL)-induced platelet activation. In contrast, extracellular signal-regulated kinase 5 (ERK5) selectively mediates ox-LDL-induced platelet activation without affecting normal hemostatic function.[8] Although the downstream MAPK effectors are increasingly well characterized, the upstream regulators that direct these pathways toward distinct functional outcomes remain largely unexplored.

The germinal center kinase (GCK)-IV family, comprising misshapen-like kinase 1 (MINK1), Traf2/Nck-interacting kinase (TNIK), and mitogen-activated protein kinase kinase kinase kinase 4 (MAP4K4), represents a group of MAP4Ks that regulate diverse cellular processes through MAPK pathway activation.[9] Beyond their canonical roles in MAPK signaling, these kinases engage in cross talk with other pathways, including Hippo[10] and transforming growth factor β/Smad pathways.[11] Our previous work demonstrated that MINK1 regulates platelet dense granule secretion through p38 and ERK1/2 activation.[12] MAP4K4 activity is regulated by receptor tyrosine kinase, small GTPases, and protein phosphatase 2A.[13] Upon activation, MAP4K4 directly phosphorylates mixed lineage kinase 3 (MLK3),[14] thereby activating the JNK signaling pathway. Despite lack of genetic ablation models of MAP4K4, pharmacological inhibition of MAP4K4 has been reported to attenuate the activation of ERK1/2, p38 and JNK, and to subsequently reduce platelet aggregation, TXA2 production, and αIIbβ3 activation.[15] However, the potential roles of the other GCK family member TNIK in platelet function remain unexplored.

TNIK represents a particularly intriguing candidate for investigation given its established roles in diverse physiological and pathophysiological processes,[16-18] especially in metabolic regulation. Recent studies have shown that global TNIK deficiency protects against diet-induced obesity, enhances glucose metabolism, and reduces hepatic steatosis.[19] Given the well-documented links between metabolic disorders and thrombotic complications, we hypothesized that platelet TNIK might function as a molecular switch that integrates metabolic signals with thrombotic responses. However, the specific contribution of platelet TNIK to hemostasis and thrombosis, particularly under hyperlipidemic conditions, has not been investigated.

In this study, we employed megakaryocyte/platelet-specific TNIK knockout (KO) mice to delineate the role of TNIK in platelet function. We demonstrate that TNIK promotes normal hemostasis by enhancing dense granule secretion through JNK pathway activation, while simultaneously acting as a negative regulator of hyperlipidemia-associated thrombosis by suppressing the protein kinase C ε (PKCε)/NADPH oxidase 2 (NOX2)/reactive oxygen species (ROS)/ERK5 signaling cascade. These findings reveal TNIK as a critical molecular switch that allows platelets to maintain hemostatic competence while preventing pathological thrombosis in metabolic disease states.

Methods

Animal studies

ApoE-deficient (*Apoe*$^{-/-}$) mice and *PF4-Cre*$^{+}$ mice were from the Model Animal Research Center of Nanjing University (Nanjing, China). *Tnik*$^{flox/flox}$ mice were generated by flanking the exon 6 of the *Tnik* gene with LoxP sites. Megakaryocyte/platelet-specific TNIK KO mice were generated by crossing *PF4-Cre*$^{+}$ mice with *Tnik*$^{flox/flox}$ mice. All mice used in the experiments were aged 8 to 16 weeks, with weight and sex matched across groups.

Intravital microscopy of $FeCl_3$-injured thrombus formation in mouse mesenteric arteriole

Arterial thrombosis was induced according to published protocols.[12] Calcein (10 μM)-labeled fluorescent platelets (10^8) were injected via the tail vein. The mesentery was exposed and placed on a translucent stage for fluorescence microscopy. Mesenteric arteriole injury (diameter, 60-80 μm) was induced by topical application of 10% $FeCl_3$ for 3 minutes and monitored for 60 minutes or until occlusion (blood flow cessation for >1 minute).

Tail-bleeding time assay

The tails of anesthetized mice were cut 0.5 cm from the tip and immersed in 37°C saline. Bleeding time was recorded as the duration until bleeding ceased (no flow for 1 minute). SSO (sulfo-N-succinimidyl oleate) was emulsified in 0.5% methyl cellulose and administered by oral gavage at the dose of 50 mg/kg 2 hours before the experiment.[20] Assays were terminated at 900 seconds if bleeding persisted.

Preparation of washed mice platelet

Whole blood was collected from the inferior vena cava into acid-citrate-dextrose (ACD) buffer (1/9 volume-to-volume ratio; 75 mM sodium citrate, 39 mM citric acid, and 135 mM dextrose, pH 6.5) and diluted at a 1:3 ratio with modified Tyrode's buffer (20 mM HEPES [N-2-hydroxyethylpiperazine-N'-2-ethanesulfonic acid], 137 mM NaCl, 13.8 mM $NaHCO_3$, 2.5 mM KCl, 0.36 mM NaH_2PO_4, and 5.5 mM glucose, pH 7.4). This diluted blood was then centrifuged at 180*g* for 10 minutes at room temperature to obtain platelet-rich plasma. The platelet-rich plasma was further diluted with ACD buffer (1/9 volume-to-volume ratio) and centrifuged at 700*g* for 10 minutes. Subsequently, the platelet pellet was resuspended in modified Tyrode's buffer.

Thrombus formation under flow conditions in vitro

Thrombus formation was assessed using BioFlux 200 system (Fluxion, San Francisco, CA). Microfluidic plates were coated overnight with fibrillar collagen at a concentration of 100 μg/mL. Heparin (7.5 IU/mL)-anticoagulated mouse whole blood or reconstituted whole blood was perfused over collagen-coated surface for 5 minutes at shear rates of 1000 s^{-1}. Thrombus formation and platelet adhesion were visualized using an inverted fluorescence microscope (magnification ×20 and 0.4 numerical aperture). Images were acquired with a Nikon DS-Qi1-U3 CCD camera, and the platelet-covered area was measured using BioFlux software (Fluxion, San Francisco, CA).

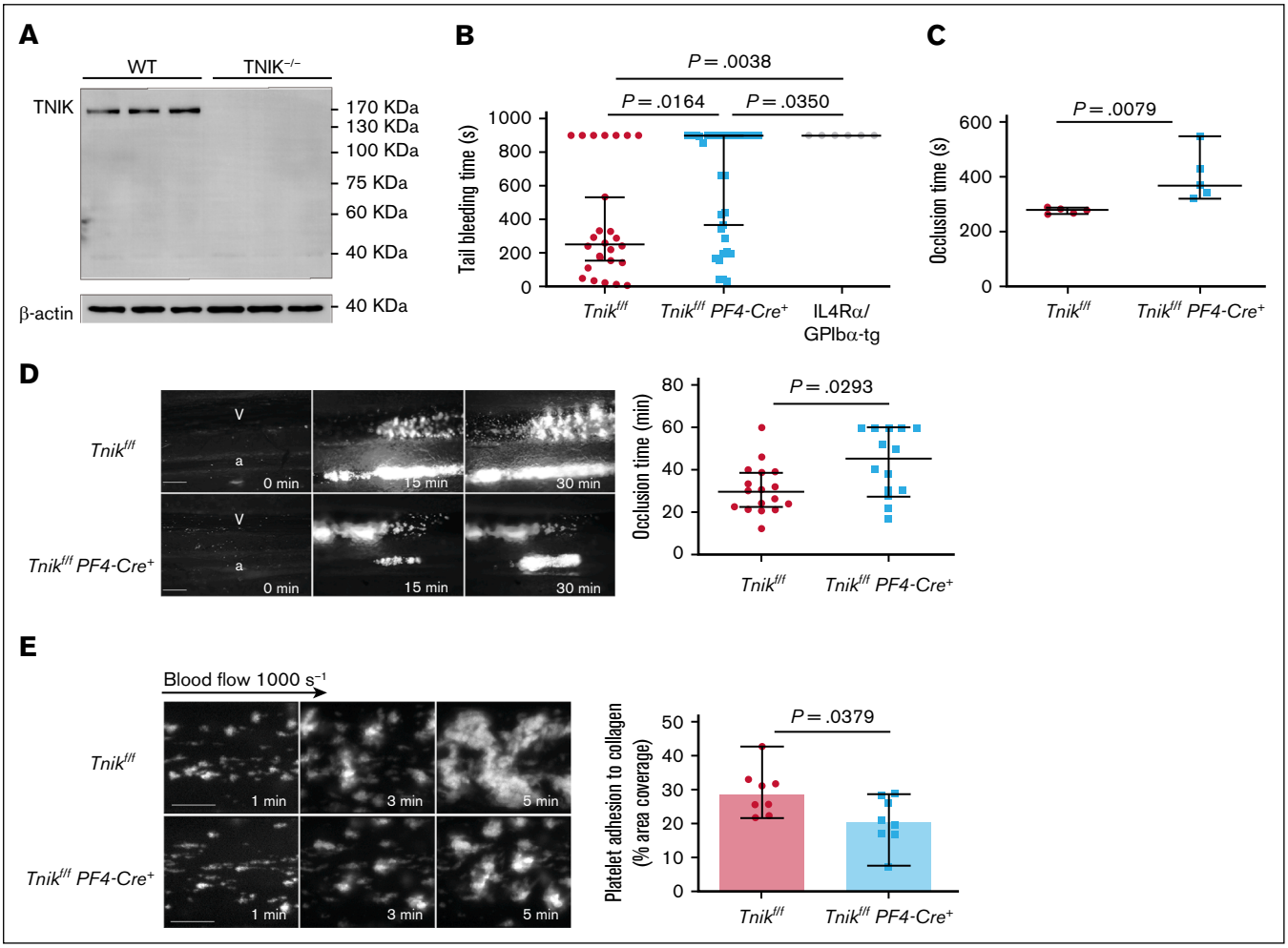

Figure 1. TNIK deficiency impairs hemostasis and arterial thrombus formation. (A) Western blot confirmation of TNIK deletion in platelets. (B) Tail bleeding times in WT (n = 26), TNIK$^{-/-}$ mice (n = 34), and IL4RAα/GPIbα-tg mice (n = 6). (C) Time to occlusion after $FeCl_3$-induced carotid artery injury (n = 5 per group). (D) Representative images of thrombus formation in $FeCl_3$-injured mesenteric arterioles at indicated time points (scale bar, 200 μm) and quantification of occlusion time (WT, n = 17; TNIK$^{-/-}$, n = 14). (E) In vitro thrombus formation on collagen-coated surfaces under arterial shear conditions (1000 s^{-1}) with representative images and quantification of thrombus area coverage (n = 8 per group; scale bar, 100 μm). Data represent median with 95% confidence interval (CI; 2-tailed Mann-Whitney test).

Table 1. Hematologic analysis

	WT	TNIK$^{-/-}$	ApoE WT	ApoE TNIK$^{-/-}$
RBCs, $\times 10^{12}$/L	9.253 ± 0.2267	9.405 ± 0.1353	7.881 ± 0.2225‡	8.035 ± 0.2579*
WBCs, $\times 10^{9}$/L	7.025 ± 0.5844	8.135 ± 0.7413	6.239 ± 2.030	3.862 ± 0.4879‡
PLTs, $\times 10^{9}$/L	903.3 ± 34.85	909.2 ± 57.90	877.0 ± 79.39	919.3 ± 59.63
HCT, %	45.53 ± 0.7969	44.87 ± 0.9979	37.74 ± 0.9710‡	39.12 ± 1.112*
HGB, g/dL	13.33 ± 0.2186	13.45 ± 0.1910	11.07 ± 0.3220‡	11.58 ± 0.3250*
MPV, fL	8.483 ± 0.1376	8.200 ± 0.07303	8.429 ± 0.1911	7.917 ± 0.08724*,†

Data are presented as mean ± standard error of the mean. No abnormalities or significant differences in hematologic parameters were found between WT and TNIK$^{-/-}$ mice under control diet conditions (n = 6-7; 2-tailed Mann-Whitney test).

HCT, hematocrit; HGB, hemoglobin; MPV, mean platelet volume; PLT, platelet; RBC, red blood cell; WBC, white blood cell.

*Significant at the 0.05 probability level compared to WT in the normal control group.

†Significant at the .05 probability level compared to ApoE WT in the BMT group.

‡Significant at the .01 probability level compared to WT in the normal control group.

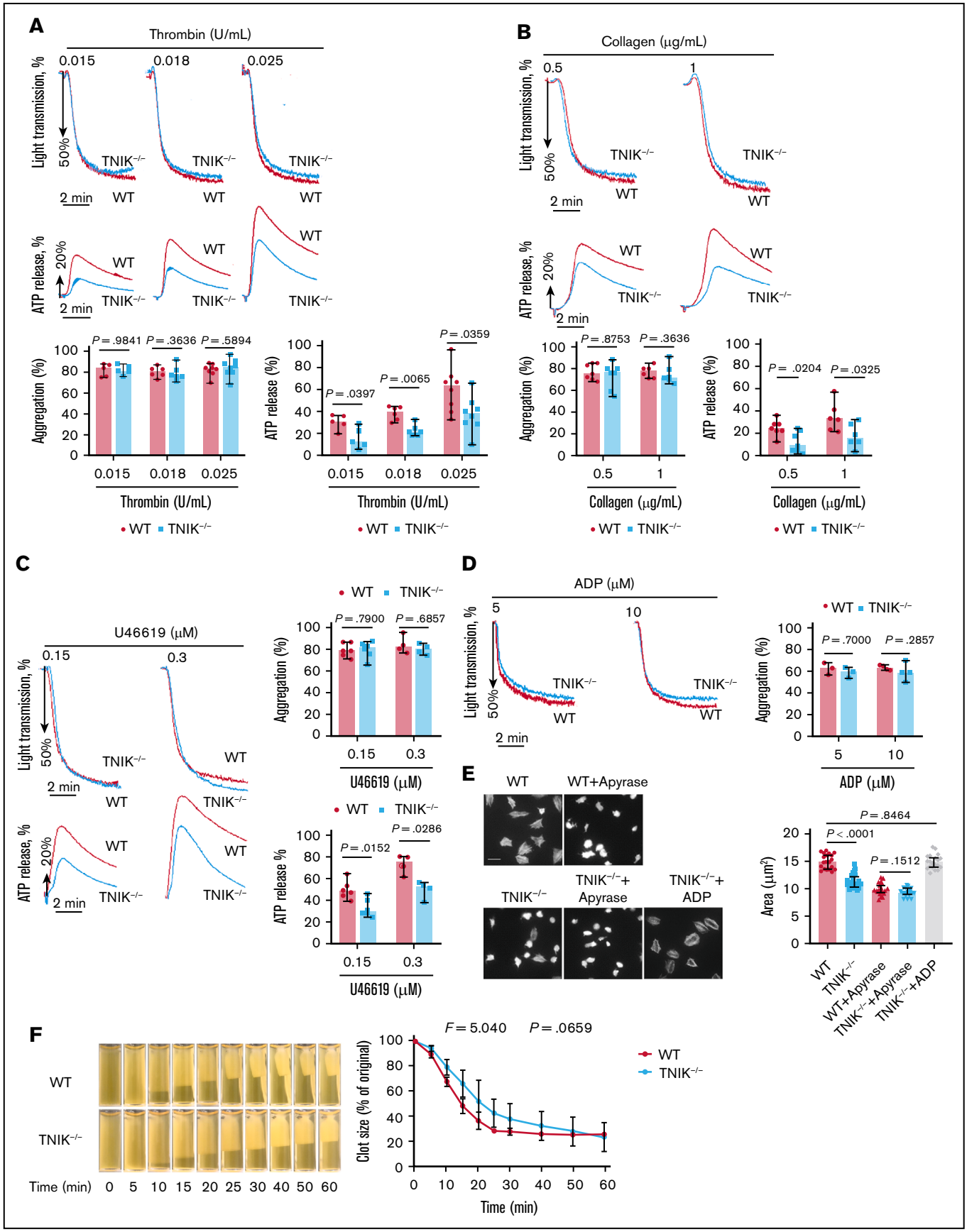
A
Thrombin (U/mL)
0.015
0.018
0.025
Light transmission, %
50%
TNIK−/−
WT
2 min
ATP release, %
20%
Aggregation (%)
ATP release (%)
P = .9841
P = .3636
P = .5894
P = .0397
P = .0065
P = .0359
Thrombin (U/mL)
WT
TNIK−/−
B
Collagen (μg/mL)
0.5
1
P = .8753
P = .3636
P = .0204
P = .0325
Collagen (μg/mL)
C
U46619 (μM)
0.15
0.3
P = .7900
P = .6857
P = .0152
P = .0286
D
ADP (μM)
5
10
P = .7000
P = .2857
E
WT
WT+Apyrase
TNIK−/−
TNIK−/−+ Apyrase
TNIK−/−+ ADP
P = .8464
P < .0001
P = .1512
Area (μm²)
WT
TNIK−/−
WT+Apyrase
TNIK−/−+Apyrase
TNIK−/−+ADP
F
Time (min)
0 5 10 15 20 25 30 40 50 60
F = 5.040
P = .0659
Clot size (% of original)

Figure 2.

Platelet aggregation and ATP secretion

Platelet aggregation and ATP secretion assays were conducted using a lumi-aggregometer (Chrono-Log, Havertown, PA) at 37°C with stirring (1200 revolutions per minute). Washed platelets (200×10^9/L) in modified Tyrode's buffer were stimulated with thrombin, collagen, U46619, and ADP (in the presence of fibrinogen). ATP release was measured using luciferin-luciferase reagent. Inhibitors were preincubated with the platelets for 5 minutes before stimulation.

Platelet spreading on fibrinogen

Glass coverslips were coated with fibrinogen (20 μg/mL) in 0.1 M $NaHCO_3$ (pH 8.3) overnight at 4°C. Platelets (20×10^9/L) were incubated on fibrinogen-coated surfaces at 37°C for 60 minutes, with or without prior treatment with 0.1 U/mL apyrase or 1 mM ADP for 5 minutes. After 3 washes with phosphate-buffered saline, the platelets were fixed, permeabilized, and stained with fluorescein-labeled phalloidin. Adherent platelets were imaged by an inverted fluorescence microscope (Nikon Ti-S) equipped with an S Plan Fluor lens (magnification ×100 and 1.30 numerical aperture oil objective). Images were captured using a Nikon DS-Qi1-U3 camera and quantified with NIS-Elements software (Nikon, Tokyo, Japan).[21]

Measurement of intracellular ROS

Intracellular ROS was measured according to a previously reported method.[22] Briefly, washed platelets (100×10^9/L) were incubated for 15 minutes at 37°C with fluorogenic probe H2DCF-DA (2',7'-dichlorofluorescein diacetate; 50 μM), followed by stimulation with ox-LDL for 10 minutes at 37°C in darkness. Samples were diluted with 10-fold phosphate-buffered saline containing 50 μM H2DCF-DA and were analyzed by flow cytometry immediately.

Serotonin content and release assay

The platelet pellet was resuspended in 200-μL double-distilled water and vigorously vortexed to lyse the cells and release its contents. Platelet 5-hydroxytryptamine (5-HT) content was determined according to the instructions of the enzyme-linked immunosorbent assay kit, and detection was performed using an M5 microplate reader (Molecular Devices, San Jose, CA).

Immunoprecipitation (IP) and liquid chromatography–tandem mass spectrometry

Platelets were lysed using 1% NP-40. Cell lysate was incubated with primary antibodies or control immunoglobulin G at 4°C overnight. The next day, protein A/G agarose beads were added to the suspension and incubated at 4°C for an additional 4 hours. Bound proteins were eluted with 2× loading buffer and analyzed by immunoblotting or subjected to mass spectrometry-based proteomic sequencing.

Statistical analysis

The data are presented as either the median with 95% confidence interval (CI) or the mean ± standard error of the mean (SEM). We analyzed statistical significance with paired Student *t* test, 2-tailed Mann-Whitney *U* test, and 2-way analysis of variance, as specified in the figure legends. Analyses were performed using GraphPad Prism 8 (GraphPad Software, San Diego, CA). Bioinformatic analysis of the proteomic data was performed using R Studio software (Posit, Boston, MA).

All animal protocols were approved by Zhejiang University Laboratory Animal Welfare and Ethics Committee.

Results

Platelet-specific TNIK deficiency does not affect platelet development or surface receptor expression

We generated megakaryocyte/platelet-specific TNIK KO mice (*Tnik*$^{flox/flox}$ *PF4-Cre*$^+$; hereafter TNIK$^{-/-}$) and confirmed TNIK deletion by western blot analysis (Figure 1A). These mice developed normally with no spontaneous bleeding or thrombotic events. Hematologic parameters, including platelet counts, mean platelet volume, and blood cell counts, were comparable between TNIK$^{-/-}$ and wild-type (WT) littermates (Table 1). Electron microscopy revealed normal platelet ultrastructure and α-granule content in TNIK$^{-/-}$ mice (supplemental Figure 1A). Flow cytometry confirmed equivalent surface expression of key platelet receptors glycoprotein VI, CD41 (integrin αIIb), and CD42b (GPIbα) between genotypes (supplemental Figure 1B).

TNIK deficiency impairs hemostasis and arterial thrombus formation

To assess the role of TNIK in hemostasis, we performed tail bleeding assays. TNIK$^{-/-}$ mice exhibited significantly prolonged bleeding times compared to WT controls (WT, 252s [95% CI, 247.7-521.6s] vs TNIK$^{-/-}$, 898s [95% CI, 509.3-743.9s]), with IL4RAα/GPIbα-tg mice included as a positive control (Figure 1B). In $FeCl_3$-induced arterial thrombosis models, TNIK$^{-/-}$ mice showed markedly delayed occlusive thrombus formation in both carotid (WT, 279s [95% CI, 263.5-289.7s] vs TNIK$^{-/-}$, 368s [95% CI, 288.8-515.6s]) and mesenteric arterioles (WT, 29.83min [95% CI, 24.91-36.7min] vs TNIK$^{-/-}$, 45.21min [95% CI, 34.35-52.61min]; Figure 1C-D). In vitro thrombus formation under arterial shear conditions (1000 s^{-1}) revealed ~30% reduction in thrombus area coverage for TNIK$^{-/-}$ platelets (Figure 1E). These data suggested a significant role of TNIK in hemostasis and thrombosis. To more accurately evaluate the initial platelet adhesion process, we established a reconstituted whole blood system with reduced platelet counts (20×10^9/L) in the perfusion assay. Initial platelet adhesion remained intact in TNIK$^{-/-}$ platelets (supplemental Figure 2), suggesting that TNIK primarily regulates thrombus growth rather than initial adhesive events.

Platelet TNIK regulates dense granule secretion

To identify the cellular basis for the hemostatic defect, we examined platelet functional responses. TNIK$^{-/-}$ platelets exhibited normal aggregation rates in response to thrombin, collagen, TXA_2 analog U46619, and ADP but showed markedly reduced ATP

Figure 2. TNIK regulates platelet dense granule secretion without affecting aggregation. (A-D) Representative traces and quantification of platelet aggregation and ATP release in response to indicated agonists. (E) Platelet spreading on immobilized fibrinogen with or without apyrase (0.1 U/mL) or ADP (1 μM); representative images (scale bar, 10 μm) and quantification of spreading area. Data represent median with 95% CI (2-tailed Mann-Whitney test). (F) Clot retraction in platelet-rich plasma at indicated time points. Data represent median with 95% CI (2-way analysis of variance).

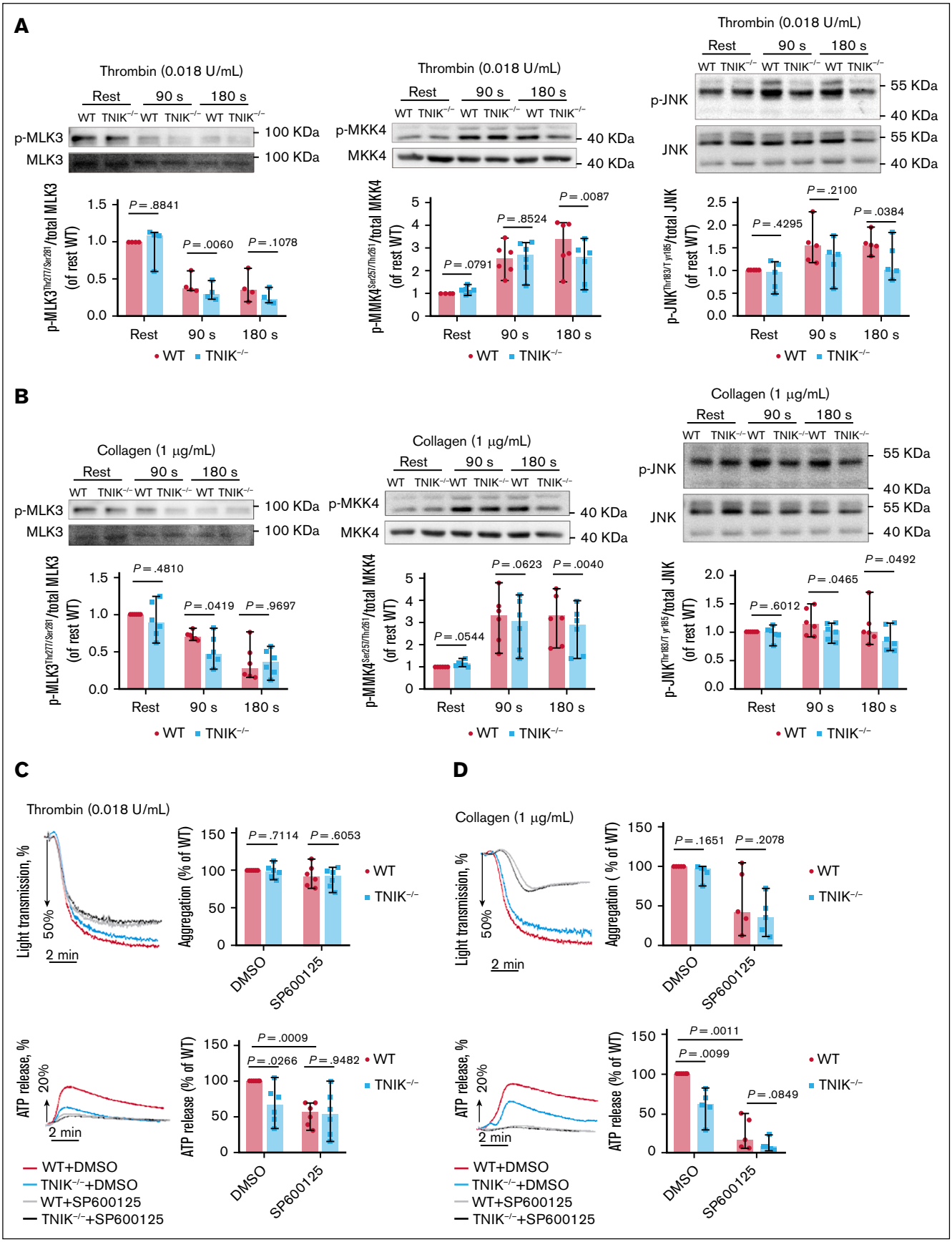
A
Thrombin (0.018 U/mL)
Rest
90 s
180 s
WT TNIK−/− WT TNIK−/− WT TNIK−/−
p-MLK3
MLK3
100 KDa
100 KDa
p-MKK4
MKK4
40 KDa
40 KDa
p-JNK
JNK
55 KDa
40 KDa
55 KDa
40 KDa
p-MLK3Thr277/Ser281/total MLK3 (of rest WT)
P = .8841
P = .0060
P = .1078
p-MMK4Ser257/Thr261/total MKK4 (of rest WT)
P = .0791
P = .8524
P = .0087
p-JNKThr183/Tyr185/total JNK (of rest WT)
P = .4295
P = .2100
P = .0384
Rest
90 s
180 s
WT
TNIK−/−
B
Collagen (1 μg/mL)
p-MLK3Thr277/Ser281/total MLK3 (of rest WT)
P = .4810
P = .0419
P = .9697
p-MMK4Ser257/Thr261/total MKK4 (of rest WT)
P = .0544
P = .0623
P = .0040
p-JNKThr183/Tyr185/total JNK (of rest WT)
P = .6012
P = .0465
P = .0492
C
Thrombin (0.018 U/mL)
Light transmission, %
50%
2 min
Aggregation (% of WT)
P = .7114
P = .6053
DMSO
SP600125
ATP release, %
20%
ATP release (% of WT)
P = .0009
P = .0266
P = .9482
WT+DMSO
TNIK−/−+DMSO
WT+SP600125
TNIK−/−+SP600125
D
Collagen (1 μg/mL)
Aggregation (% of WT)
P = .1651
P = .2078
P = .0011
P = .0099
P = .0849

Figure 3.

secretion (Figure 2A-D). Because ADP released from dense granules activates $P2Y_{12}$ receptors to amplify platelet responses, we next examined whether TNIK deficiency also affects $P2Y_{12}$ signaling directly. We examined vasodilator-stimulated phosphoprotein (VASP) dephosphorylation as a marker of $P2Y_{12}$ activation. $TNIK^{-/-}$ platelets did not exhibit differences in ADP-induced $VASP^{Ser157}$ dephosphorylation compared with WT platelets (supplemental Figure 3A), indicating that TNIK does not participate in intrinsic $P2Y_{12}$ signaling. However, after thrombin or collagen stimulation, $TNIK^{-/-}$ platelets showed impaired $VASP^{Ser157}$ dephosphorylation, compared with WT platelets, and this difference was abolished by pretreatment with the $P2Y_{12}$ inhibitor ticagrelor (supplemental Figure 3B-C). These data suggest that the physiological role of TNIK is to regulate dense granule release and thereby modulate the availability of ADP upon platelet activation. Total dense granule content (measured by high-dose thrombin stimulation), 5-HT levels, and P-selectin expression remained normal in $TNIK^{-/-}$ platelets (supplemental Figure 4A-C), indicating a specific defect in secretion mechanism rather than granule biogenesis. Flow cytometry revealed normal integrin $\alpha IIb\beta 3$ activation (JON/A binding) in $TNIK^{-/-}$ platelets (supplemental Figure 4D), suggesting that TNIK may not be directly involved in "inside-out" signaling. However, $TNIK^{-/-}$ platelets demonstrated significantly impaired spreading on immobilized fibrinogen ($11.17 \pm 0.12\ \mu m^2$ vs $14.73 \pm 0.16\ \mu m^2$; Figure 2E). This defect was partially rescued by exogenous ADP addition and was completely normalized by apyrase treatment (Figure 2E). Clot retraction was only slightly delayed in $TNIK^{-/-}$ platelets without affecting the final clot volume (Figure 2F). Nevertheless, TNIK ablation in platelets did not alter the phosphorylation of $\beta 3^{Tyr747}$, $\beta 3^{Tyr759}$, and Src^{Tyr416} provoked by Mn^{2+} stimulation (supplemental Figure 4E). These results confirm that TNIK deficiency impairs dense granule secretion rather than causing intrinsic integrin signaling defects.

TNIK selectively regulates the MLK3/MKK4/JNK signaling cascade after thrombin and collagen stimulation

Given the established role of TNIK as a MAP4K, we investigated MAPK signaling in $TNIK^{-/-}$ platelets. After thrombin or collagen stimulation, $TNIK^{-/-}$ platelets exhibited significantly reduced phosphorylation of $JNK1/2^{Thr183/Tyr185}$ and its upstream activators mitogen-activated protein kinase kinase 4 (MKK4) and MLK3 (Figure 3A-B). Treatment with the JNK inhibitor SP600125 eliminated the difference in thrombin- and collagen-induced dense granule secretion between WT and $TNIK^{-/-}$ platelets (Figure 3C-D), confirming a causal role for JNK pathway in the observed secretion defect in $TNIK^{-/-}$ platelets. Phosphorylation of other MAPK members, including apoptosis signal-regulating kinase 1, ERK1/2, p38, and Akt, remained unaffected (supplemental Figure 5), suggesting that TNIK selectively regulates the MLK3/MKK4/JNK axis.

Platelet TNIK deficiency enhances thrombosis under hyperlipidemic conditions

Given the established role of TNIK in metabolic regulation,[19] we sought to characterize its specific function in platelet activation during hyperlipidemia-associated thrombosis. We established chimeric $ApoE^{-/-}$ mice with either WT or TNIK-deficient bone marrow (Figure 4A; supplemental Figure 6A), then fed them control diet or high-fat diet (HFD) for 8 weeks. Although red blood cell count, packed cell volume, and hemoglobin levels were slightly reduced in bone marrow transplantation (BMT) groups, these parameters did not differ between WT and $TNIK^{-/-}$ mice (Table 1). Plasma levels of total cholesterol, triglyceride, low-density lipoprotein cholesterol, very low-density lipoprotein, and ox-LDL were increased in HFD-fed mice compared with control diet-fed mice (supplemental Figure 6B-F). High-density lipoprotein cholesterol levels were decreased in both groups of chimeric $ApoE^{-/-}$ mice with BMT compared with control mice expressing ApoE (supplemental Figure 6G). Comparable plasma lipid levels between WT and $TNIK^{-/-}$ mice indicated that TNIK deficiency did not influence hyperlipidemia development (supplemental Figure 6B-G). Strikingly, although $TNIK^{-/-}/ApoE^{-/-}$ mice on control diet showed prolonged bleeding times consistent with our initial findings (WT, 53s [95% CI, 42.74-484.2s] vs $TNIK^{-/-}$, 315.5s [95% CI, 248.2-690.5s), HFD-fed $TNIK^{-/-}/ApoE^{-/-}$ mice displayed significantly shortened bleeding times compared to HFD-fed $TNIK^{+/+}/ApoE^{-/-}$ controls (WT, 118.5s [95% CI, 60.11-187.9s] vs $TNIK^{-/-}$, 30s [95% CI, 5.267-85.27s]; Figure 4B). Similarly, in the $FeCl_3$-induced mesenteric arteriole thrombosis model, HFD-fed $TNIK^{-/-}/ApoE^{-/-}$ mice formed occlusive thrombi more rapidly than HFD-fed $TNIK^{+/+}/ApoE^{-/-}$ mice (WT, 16 min [95% CI, 14.6-20.6 min] vs $TNIK^{-/-}$, 11.17 min [95% CI, 9.476-13.67 min]; Figure 4C). To determine whether the enhanced thrombosis in HFD-fed $TNIK^{-/-}/ApoE^{-/-}$ mice resulted from improved dense granule secretion, we examined responses to thrombin and collagen. However, platelets from HFD-fed $TNIK^{-/-}/ApoE^{-/-}$ mice exhibited comparable thrombin- and collagen-induced aggregation and ATP release to those from HFD-fed $TNIK^{+/+}/ApoE^{-/-}$ mice (supplemental Figure 7). These results indicate that TNIK inhibits platelet activation under hyperlipidemic conditions through a distinct mechanism independent of dense granule secretion. In a whole blood perfusion assay, $TNIK^{-/-}$ platelets showed enhanced adhesion and formed larger thrombi when whole blood from regular-fed mice was supplemented with ox-LDL (Figure 4D). Furthermore, washed $TNIK^{-/-}$ platelets displayed increased aggregation in response to ox-LDL (Figure 4E). These findings reveal a multifaceted, context-dependent role for platelet TNIK: promoting hemostasis under normal conditions while inhibiting thrombosis under hyperlipidemic conditions.

TNIK inhibits ox-LDL–induced platelet activation through suppression of the PKC/NOX2/ROS/ERK5 pathway

To elucidate the mechanism underlying the inhibitory role of TNIK under hyperlipidemic conditions, we examined relevant signaling

Figure 3. TNIK selectively regulates the MLK3/MKK4/JNK signaling pathway in platelets. (A-B) Immunoblot analysis of MLK3, MKK4, and JNK phosphorylation in platelets stimulated with thrombin (0.018 U/mL) or collagen (1 μg/mL), with quantification of band intensity. (C-D) Effects of the JNK inhibitor SP600125 (10 μM) on aggregation and ATP release induced by thrombin and collagen. Data represent median with 95% CI (paired Student *t* test). DMSO, dimethyl sulfoxide.

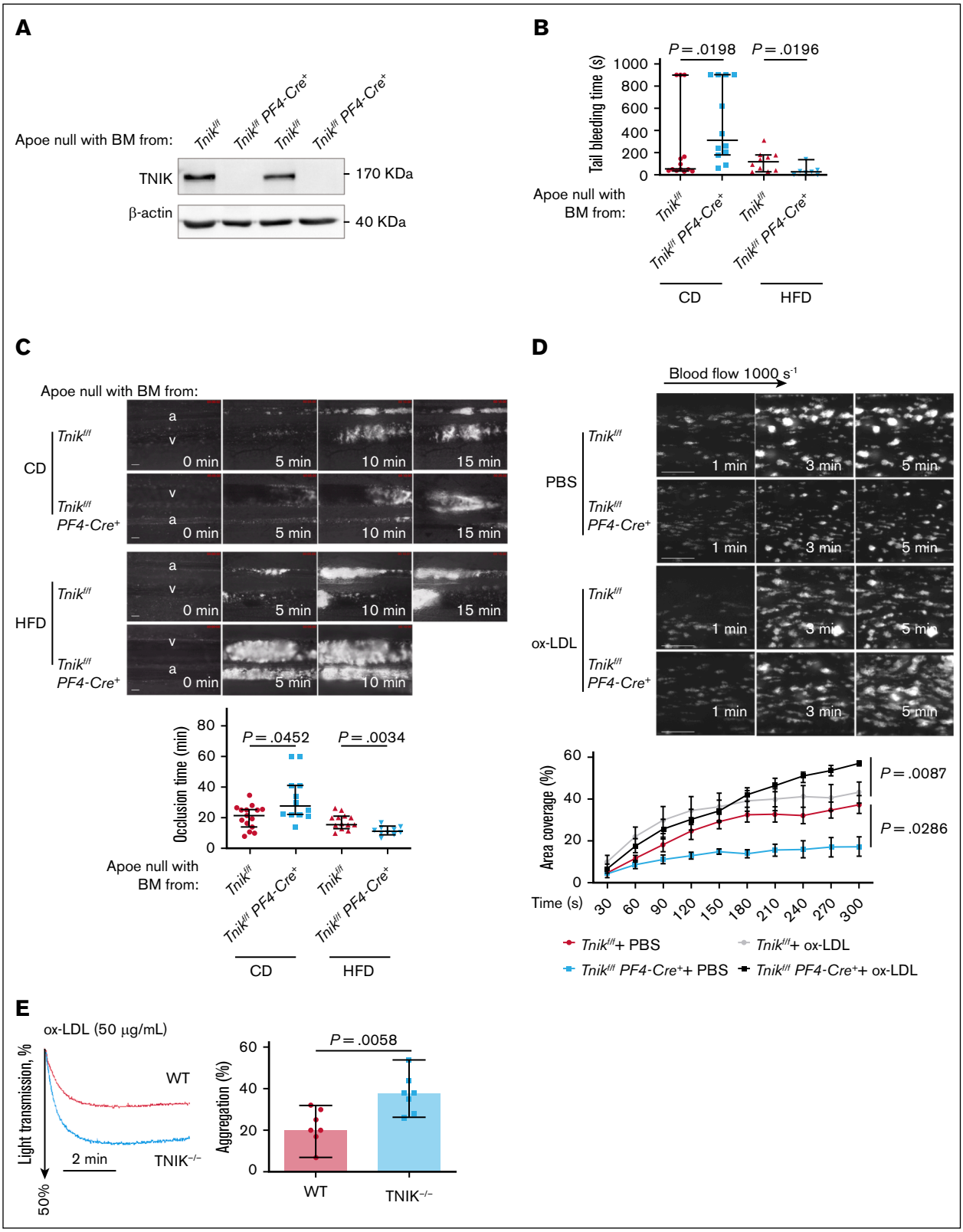

Figure 4. Platelet TNIK deficiency enhances thrombosis under hyperlipidemic conditions. (A) Western blot confirmation of TNIK deletion in platelets from BMT ApoE$^{-/-}$ mice. (B) Tail bleeding times in ApoE$^{-/-}$ mice with WT or TNIK$^{-/-}$ BM fed control diet or HFD. (C) Representative images and quantification of $FeCl_3$-induced mesenteric arteriole thrombosis in chimeric mice (scale bar, 100 μm). (D) In vitro thrombus formation on collagen with or without ox-LDL stimulation (scale bar, 100 μm). (E) Platelet aggregation in response to ox-LDL (50 μg/mL). Data represent median with 95% CI (2-tailed Mann-Whitney test). BM, bone marrow; CD, control diet; PBS, phosphate-buffered saline.

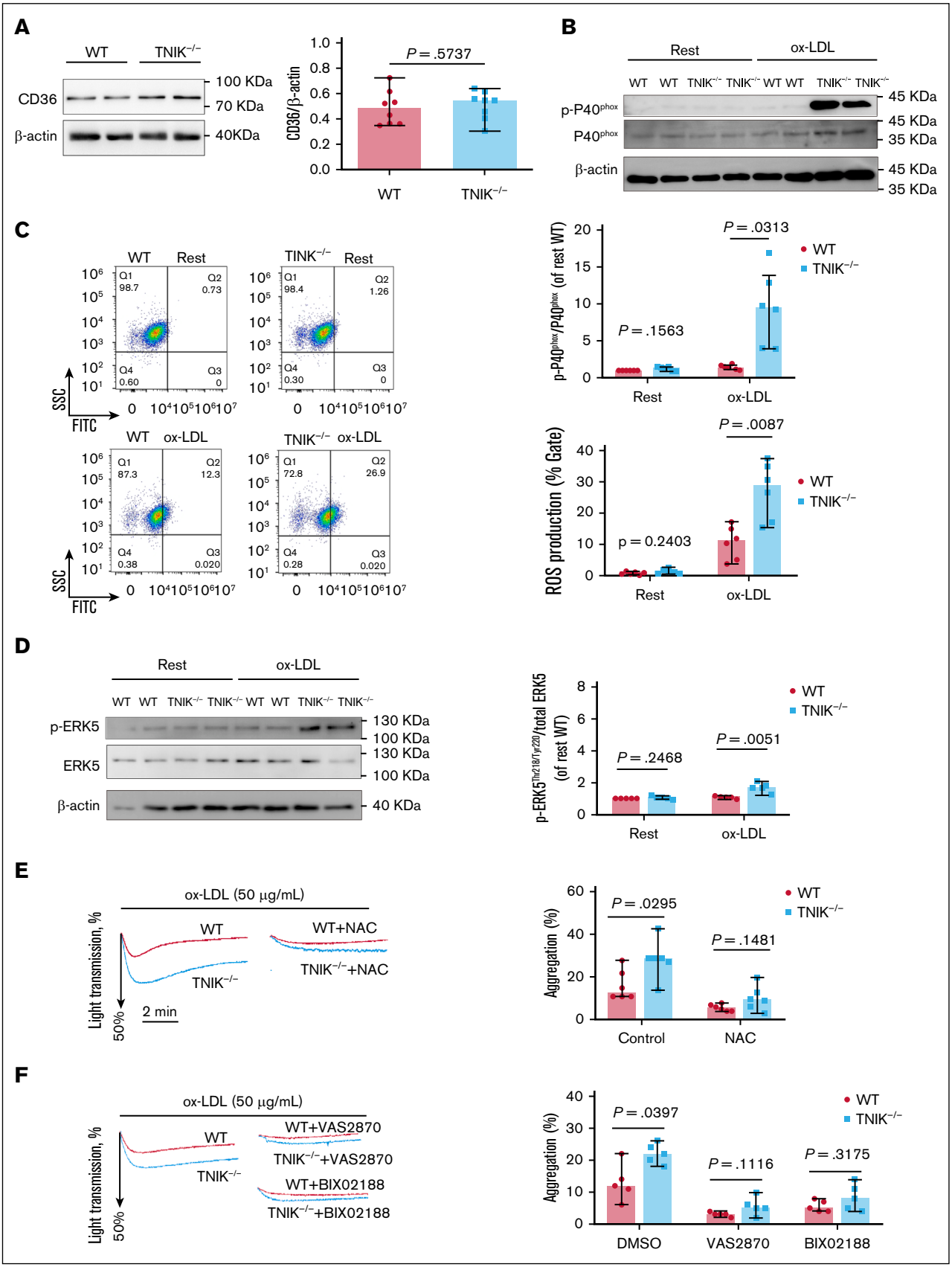
A
WT
TNIK−/−
CD36
β-actin
100 KDa
70 KDa
40KDa
CD36/β-actin
P = .5737
WT
TNIK−/−
B
Rest
ox-LDL
p-P40phox
P40phox
β-actin
45 KDa
35 KDa
C
WT Rest
TINK−/− Rest
WT ox-LDL
TNIK−/− ox-LDL
SSC
FITC
p-P40phox/P40phox (of rest WT)
P = .0313
P = .1563
ROS production (% Gate)
P = .0087
p = 0.2403
D
p-ERK5
ERK5
β-actin
130 KDa
100 KDa
40 KDa
p-ERK5Thr218/Tyr220/total ERK5 (of rest WT)
P = .2468
P = .0051
E
ox-LDL (50 μg/mL)
WT
TNIK−/−
WT+NAC
TNIK−/−+NAC
Light transmission, %
50%
2 min
Aggregation (%)
P = .0295
P = .1481
Control
NAC
F
ox-LDL (50 μg/mL)
WT+VAS2870
TNIK−/−+VAS2870
WT+BIX02188
TNIK−/−+BIX02188
P = .0397
P = .1116
P = .3175
DMSO
VAS2870
BIX02188

Figure 5.

pathways. CD36 is the pivotal contributor to platelet hyperreactivity under hyperlipidemic conditions.[2] We first confirmed that TNIK deficiency does not influence CD36 expression on platelets (Figure 5A). Downstream of CD36, the key signaling events include NOX activation and ROS generation,[2] which in turn activates downstream ERK5.[8] Upon ox-LDL stimulation, TNIK$^{-/-}$ platelets exhibited enhanced p40^{phox} phosphorylation, suggesting increased NOX2 activation compared to WT platelets (Figure 5B). Consistent with an enhanced function of NOX2, TNIK$^{-/-}$ platelets had increased ROS production (Figure 5C) and augmented ERK5$^{Thr218/Tyr220}$ phosphorylation (Figure 5D), which were revealed by flow cytometry and western blotting, respectively. Pharmacological inhibition of ROS (N-acetylcysteine; Figure 5E), NOX (VAS2870), or ERK5 (BIX02188; Figure 5F) abolished the enhanced aggregation of TNIK$^{-/-}$ platelets in response to ox-LDL, confirming the functional relevance of this pathway. Our data establish that TNIK deficiency drives platelet activation via a p40^{phox} phosphorylation and NOX2-ROS-dependent pathway, in which ROS-mediated ERK5 activation is essential for this process in response to ox-LDL. Having established that TNIK regulates the PKCε/NOX2/ROS/ERK5 pathway under ox-LDL stimulation, we next tested whether this signaling cascade occurs downstream of CD36 under hyperlipidemic conditions. SSO-mediated CD36 blockade normalized bleeding time in HFD-fed TNIK$^{-/-}$ /ApoE$^{-/-}$ mice to levels comparable to those in HFD-fed TNIK$^{+/+}$/ApoE$^{-/-}$ mice (supplemental Figure 8), confirming TNIK as a downstream regulator of CD36 under hyperlipidemic conditions.

TNIK forms distinct signaling complexes under hemostatic vs hyperlipidemic conditions

We cross validated key signaling molecules downstream of ox-LDL or thrombin treatment in platelet. TNIK deficiency did not attenuate thrombin-induced p40^{phox} phosphorylation (supplemental Figure 9A) nor enhance ox-LDL–stimulated JNK phosphorylation (supplemental Figure 9B). Even after JNK inhibitor treatment, TNIK$^{-/-}$ platelets still exhibited enhanced ox-LDL-induced aggregation than WT platelets (supplemental Figure 9C). These results suggest that TNIK diverges into 2 distinct pathways in response to hemostatic vs hyperlipidemic conditions.

To understand how TNIK mediates opposing effects in different contexts, we performed IP of platelet TNIK, followed by mass spectrometry. These analyses revealed enrichment of JNK pathway components in TNIK immunoprecipitants after thrombin stimulation (Figure 6A-B). JNK-interacting protein 1 (JIP1) interacts with multiple components of the JNK signaling pathway.[23,24] Co-IP experiments confirmed that TNIK selectively interacts with JIP1 after thrombin or collagen stimulation but not after ox-LDL treatment (Figure 6C-D). Inhibition of JIP1 with BI-78D3[25] eliminated differences in dense granule secretion (Figure 6E) and JNK phosphorylation (Figure 6F) between WT and TNIK$^{-/-}$ platelets.

Consistent with enhanced phosphorylation of p40^{phox}, we observed that ox-LDL induced an increase of ~40 kDa in the phosphorylation of PKC substrates in TNIK$^{-/-}$ platelets (Figure 7A). These data suggest a model in which TNIK may suppress NOX2 activation by interacting with PKC. TNIK bound to multiple PKC isoforms under ox-LDL stimulation; however, only its interaction with PKCε exhibited a distinct pattern, being specifically induced by ox-LDL but not thrombin. (Figure 7B-C). Furthermore, PKCε phosphorylation at Ser729 was elevated in TNIK$^{-/-}$ platelets after ox-LDL treatment (Figure 7D). PKCε-specific inhibitor Epsilon-V1-2 attenuated ox-LDL-induced aggregation (Figure 7E) and p40^{phox} phosphorylation (Figure 7F) in TNIK$^{-/-}$ platelets. These findings establish that TNIK functions as a molecular switch, forming distinct signaling complexes that promote hemostasis through JIP1/JNK activation while preventing hyperlipidemia-associated thrombosis by inhibiting PKCε/NOX2/ROS/ERK5 signaling.

Discussion

In this study, we identified TNIK as an important molecular switch that simultaneously promotes physiological hemostasis while preventing pathological thrombosis under hyperlipidemic conditions. Using megakaryocyte/platelet-specific TNIK KO mice, we demonstrated that TNIK deficiency impairs normal hemostasis and thrombus formation, primarily due to defective dense granule secretion. However, under hyperlipidemic conditions, TNIK deficiency paradoxically enhances platelet activation and accelerates thrombosis. These opposing phenotypes reflect the ability of TNIK to engage distinct signaling pathways in response to different platelet stimuli.

Our findings establish the importance of TNIK in promoting platelet activation through enhanced dense granule secretion. Despite normal granule content, intact integrin αIIbβ3 activation, and surface expression of CD62P, TNIK$^{-/-}$ platelets exhibited markedly decreased ATP release in response to various agonists. As a result of this selective controlled release of dense granule content (eg, ADP), TNIK deletion in platelets primarily impairs thrombus growth. Consistent with the established role of GCK-IV family kinases in JNK signaling pathways,[17,24] we identified TNIK as a selective upstream activator of the MLK3-MKK4-JNK axis after thrombin or collagen activation. Consistent with a previous study,[7] JNK was shown to enhance platelet dense granule secretion. The JNK inhibitor SP600125 eliminated differences in dense granule secretion between WT and TNIK$^{-/-}$ platelets, confirming that JNK plays an essential role downstream of TNIK in response to hemostatic stimulation. These findings complement our previous work on MINK1, another GCK-IV family member that promotes platelet dense granule secretion via p38 and ERK1/2 pathways.[12] Together, these data suggest that GCK-IV kinases orchestrate platelet dense granule secretion through distinct but complementary MAPK pathways.

Figure 5. TNIK deficiency enhances PKC/NOX2/ROS/ERK5 signaling in response to ox-LDL. (A-B) Immunoblot analysis of CD36 and p40^{phox} phosphorylation in ox-LDL-stimulated platelets. Data represent median with 95% CI (paired Student *t* test). (C) Flow cytometric quantification of ROS production using H2DCF-DA. Data represent median with 95% CI (2-tailed Mann-Whitney test). (D) Immunoblot analysis of ERK5 phosphorylation. Data represent median with 95% CI (paired Student *t* test). (E-F) Effects of the ROS inhibitor NAC (2 mM), the NOX inhibitor VAS2870 (5 μM), and the ERK5 inhibitor BIX02188 (10 μM) on ox-LDL-induced platelet aggregation. Data represent median with 95% CI (2-tailed Mann-Whitney test). FITC, fluorescein isothiocyanate; SSC, side scatter.

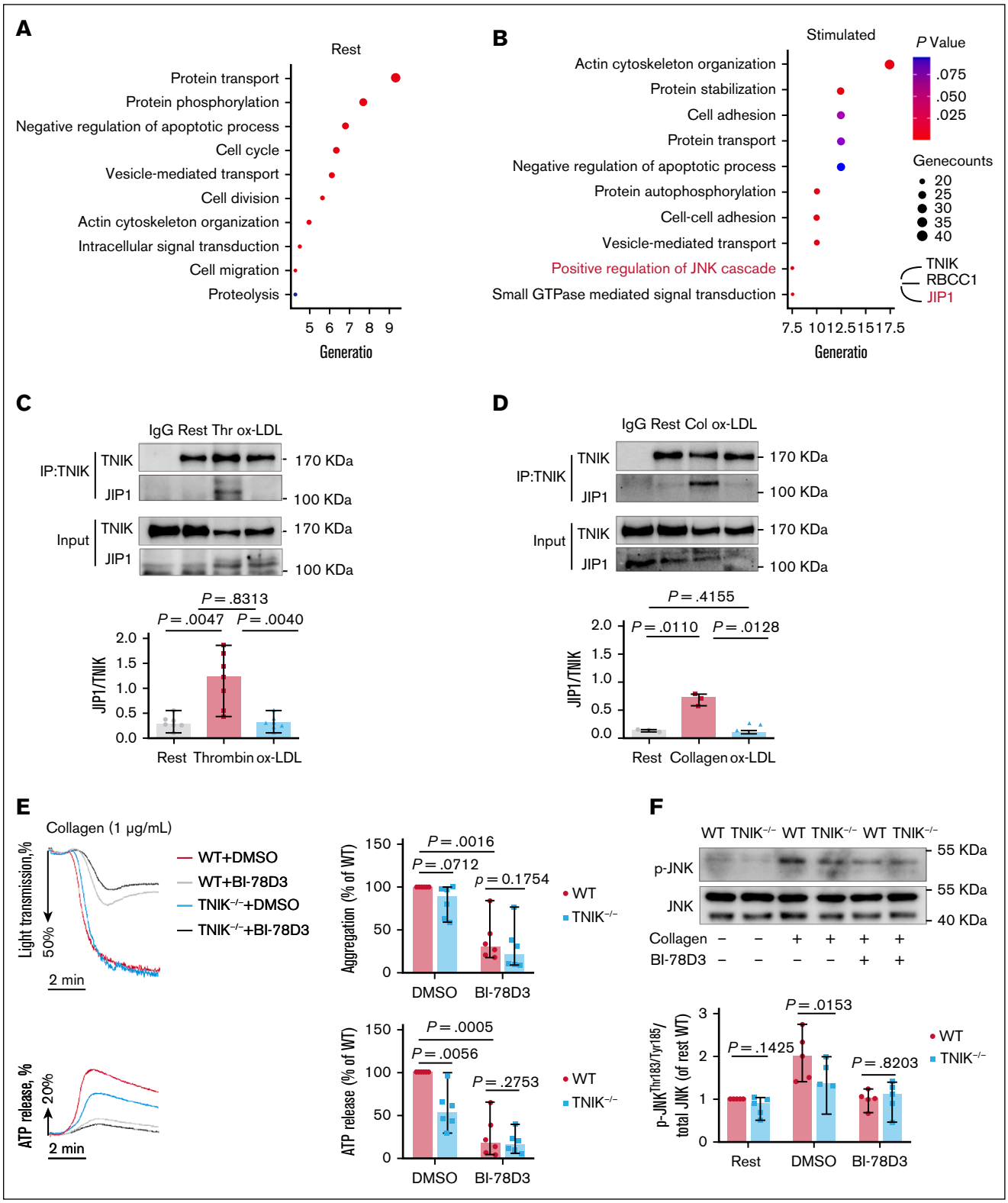

Figure 6. TNIK forms a complex with JIP1 to promote hemostatic platelet activation. (A-B) Enrichment analysis of TNIK-interacting proteins identified by mass spectrometry after thrombin stimulation. (C-D) Co-IP and immunoblot analysis of TNIK-JIP1 interaction under various stimulation conditions. Data represent median with 95% CI (2-tailed Mann-Whitney test). (E) Effects of the JIP1 inhibitor BI-78D3 on collagen-induced ATP release. (F) Effects of BI-78D3 on JNK phosphorylation. Data represent median with 95% CI (paired Student *t* test). DMSO, dimethyl sulfoxide; IgG, immunoglobulin G; kDa, kilodalton.

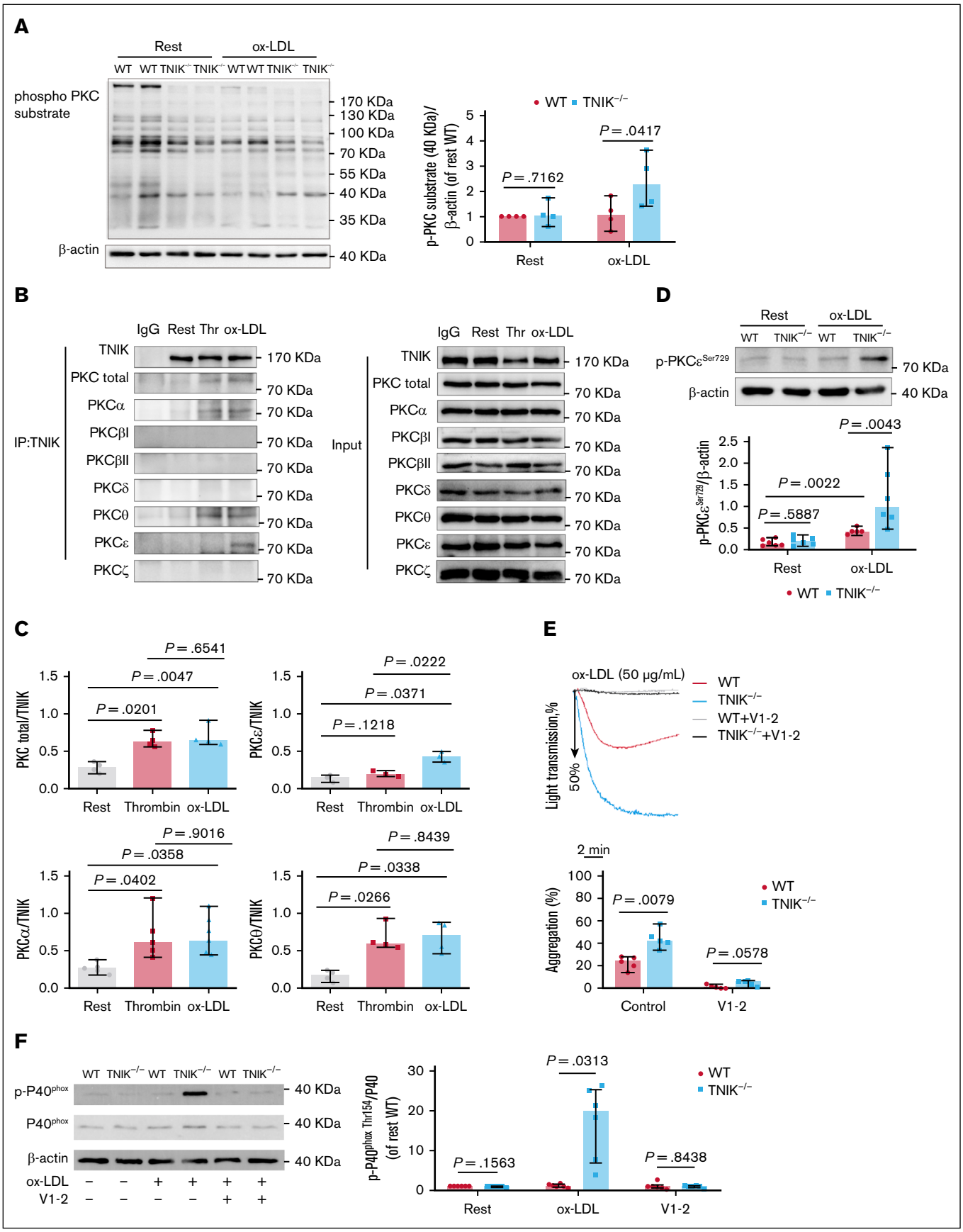
A
Rest
ox-LDL
WT WT TNIK−/− TNIK−/− WT WT TNIK−/− TNIK−/−
phospho PKC substrate
170 KDa
130 KDa
100 KDa
70 KDa
55 KDa
40 KDa
35 KDa
β-actin
40 KDa
WT TNIK−/−
P = .7162
P = .0417
p-PKC substrate (40 KDa)/ β-actin (of rest WT)
Rest
ox-LDL
B
IgG Rest Thr ox-LDL
IP:TNIK
Input
TNIK
PKC total
PKCα
PKCβI
PKCβII
PKCδ
PKCθ
PKCε
PKCζ
170 KDa
70 KDa
D
Rest
ox-LDL
WT TNIK−/− WT TNIK−/−
p-PKCε Ser729
β-actin
70 KDa
40 KDa
P = .0043
P = .0022
P = .5887
p-PKCε Ser729/β-actin
C
P = .6541
P = .0047
P = .0201
PKC total/TNIK
P = .0222
P = .0371
P = .1218
PKCε/TNIK
P = .9016
P = .0358
P = .0402
PKCα/TNIK
P = .8439
P = .0338
P = .0266
PKCδ/TNIK
Rest
Thrombin
ox-LDL
E
ox-LDL (50 μg/mL)
WT
TNIK−/−
WT+V1-2
TNIK−/−+V1-2
Light transmission,%
50%
2 min
Aggregation (%)
P = .0079
P = .0578
Control
V1-2
F
WT TNIK−/− WT TNIK−/− WT TNIK−/−
p-P40phox
P40phox
β-actin
40 KDa
ox-LDL
V1-2
p-P40phox Thr154/P40 (of rest WT)
P = .0313
P = .1563
P = .8438
Rest
ox-LDL
V1-2

Figure 7.

The most striking finding of our study is context-dependent function of TNIK in thrombosis. Our data reveal that platelet-specific TNIK KO accelerates thrombosis under hyperlipidemic conditions without affecting systemic lipid profiles. These results clearly demonstrate that platelets TNIK serves as a protective mechanism against hyperlipidemia-associated thrombotic complications. Mechanistically, we found that TNIK deficiency enhances ox-LDL-induced platelet activation through increased activation of the NOX2/ROS/ERK5 pathway. Previous studies have established that CD36-dependent recognition of ox-LDL triggers PKC activation, which in turn activates NOX2 to generate ROS.[2,8] Our data reveal that TNIK$^{-/-}$ platelets exhibit enhanced phosphorylation of p40^{phox}, increased ROS production, and augmented ERK5 activation in response to ox-LDL. Inhibition of NOX (VAS2870), ROS (NAC), or ERK5 (BIX02188) normalized the hyperreactive phenotype of TNIK$^{-/-}$ platelets, confirming the causal role of this pathway. It is important to note that ERK5 functions as a central integrator of multiple platelet activation pathways, including those initiated by protease-activated receptors, thromboxane receptor,[26] or GPIb-IX.[27] The selective enhancement of ERK5 activation in TNIK-deficient platelets under ox-LDL stimulation, but not with thrombin or collagen, indicates that TNIK specifically regulates the CD36/PKCε/NOX2/ERK5 axis. This stimulus-dependent regulation positions TNIK as a critical molecular switch that maintains the balance between hemostasis and pathological thrombosis.

What distinguishes TNIK from previously identified regulators of platelet function is its dual role as both a positive regulator of hemostasis and a negative regulator of pathological thrombosis. Our co-IP and mass spectrometry analyses revealed that TNIK forms distinct protein complexes depending on the stimulus. After hemostatic stimuli (thrombin or collagen), TNIK selectively interacts with JIP1, a scaffolding protein that enhances JNK signaling by facilitating proximity between JNK and its upstream kinases.[24] This interaction promotes dense granule secretion and subsequent amplification of platelet activation. However, under ox-LDL stimulation, TNIK fails to engage JIP1 but instead binds to PKCε.

The identification of PKCε as the binding partner of TNIK under hyperlipidemic conditions is particularly intriguing. PKC-induced NOX2 activation is a major driver of hyperlipidemia-induced platelet activation.[2] Among PKC isoforms, only PKCε was found to interact with TNIK in platelets stimulated with ox-LDL but not thrombin. PKCε is well documented in vascular pathology, mediating ox-LDL-induced coronary vasoconstriction[28] and resistin-driven NOX/ROS activation in vascular smooth muscle cells.[29] However, the function of PKCε in platelets remains largely uncertain and understudied. The role of platelet PKCε in response to hemostatic stimuli remains controversial, with some studies reporting that PKCε positively regulates glycoprotein VI-mediated responses but not ADP/AYPGKF signaling,[30,31] whereas others report the opposite.[32] Additionally, its function under hyperlipidemic conditions has not been fully elucidated. In our study, TNIK-deficient platelets exhibited enhanced phosphorylation of PKCε at Ser729 after ox-LDL stimulation. Importantly, treatment with the PKCε-specific inhibitor Epsilon-V1-2 effectively normalized both platelet aggregation and p40^{phox} phosphorylation. These findings suggest that TNIK negatively regulates PKCε activity through direct interaction, thereby dampening downstream NOX2/ROS/ERK5 signaling.

The identification of TNIK as a "molecular switch" governing the balance between hemostasis and thrombosis offers both therapeutic opportunities and challenges. TNIK is broadly expressed across bone marrow cell populations and has been suggested as a key target in the treatment for chronic myelogenous leukemia[33] and plasma cell dyscrasias.[34] Moreover, a TNIK inhibitor (INS018_55) is currently in phase 2 trials for idiopathic pulmonary fibrosis.[35] Although these clinical studies underscore TNIK's therapeutic potential as a druggable target, our findings reveal dual and context-dependent effects on both thrombosis and hemostasis. Consequently, drug development targeting TNIK necessitates more rigorous evaluation to balance its beneficial and detrimental effects in different disease contexts. In patients with preexisting hyperlipidemia, TNIK inhibition might exacerbate thrombotic risk, whereas in normolipidemic individuals, it could precipitate bleeding complications.

Despite the significant insights provided by our study, several limitations should be acknowledged. First, the precise upstream mechanisms that determine divergent functions of TNIK remain unresolved. It is unclear what preconditions (eg, posttranslational modifications, cofactor recruitment, or subcellular localization) dictate interactions between TNIK and molecular partners. Second, although our BMT approach effectively isolated platelet-specific effects, potential contributions from other hematopoietic cells cannot be entirely excluded.

In summary, we have identified TNIK as a critical regulator of platelet homeostasis that promotes physiological hemostasis while preventing pathological thrombosis under hyperlipidemic conditions. Through stimulus-dependent interactions with JIP1 or PKCε, TNIK selectively activates JNK signaling to enhance dense granule secretion or inhibits the NOX2/ROS/ERK5 pathway to dampen ox-LDL-induced platelet hyperreactivity. These findings advance our understanding of the molecular mechanisms governing platelet responses to metabolic stress and identify TNIK as a potential therapeutic target for thrombotic complications in metabolic disorders.

Acknowledgments

The authors thank Kaixiang Zhu for help and advice. They thank Jiajia Wang from the Core Facilities, Zhejiang University School of Medicine, for flow cytometric support and Xueping Zhou for maintaining the mouse colonies.

This study was supported by grants from the National Natural Science Foundation of China (U23A20416 and 82070138

Figure 7. TNIK interacts with PKCε to inhibit ox-LDL–induced platelet activation. (A) Immunoblot analysis of PKC substrate. (B-C) Co-IP and immunoblot analysis of TNIK interaction with PKC isoforms under various stimulation conditions. (D) Immunoblot analysis of PKCε^{Ser729} phosphorylation in ox-LDL–stimulated platelets. (E) Effects of the PKCε inhibitor Epsilon-V1-2 on ox-LDL–induced platelet aggregation. (F) Effects of Epsilon-V1-2 on p40^{phox} phosphorylation. Data represent median with 95% CI (paired Student *t* test).

[H.H.]; 82404622 [L. Li]), Zhejiang Provincial Natural Science Foundation (LZ23H080001), and Discipline Construction Funding of Innovation Institute of Basic Medical Sciences, Zhejiang University.

Authorship

Contribution: L. Li and X.C. designed and performed experiments, analyzed data, and cowrote the manuscript; J.L., X.D., and Y.S. analyzed data; L. Lu contributed reagents and expertise; H.H. conceived the study, designed experiments, supervised research, and cowrote the manuscript; and all authors reviewed the manuscript.

Conflict-of-interest disclosure: The authors declare no competing financial interests.

ORCID profile: H.H., 0000-0002-0009-8218.

Correspondence: Hu Hu, Department of Pathology and Pathophysiology and Bone Marrow Transplantation Center of the First Affiliated Hospital, Zhejiang University School of Medicine, Hangzhou 310058, People's Republic of China; email: huhu@zju.edu.cn.

References

1. Michelson AD. Antiplatelet therapies for the treatment of cardiovascular disease. *Nat Rev Drug Discov*. 2010;9(2):154-169.
2. Magwenzi S, Woodward C, Wraith KS, et al. Oxidized LDL activates blood platelets through CD36/NOX2-mediated inhibition of the cGMP/protein kinase G signaling cascade. *Blood*. 2015;125(17):2693-2703.
3. Chen K, Febbraio M, Li W, Silverstein RL. A specific CD36-dependent signaling pathway is required for platelet activation by oxidized low-density lipoprotein. *Circ Res*. 2008;102(12):1512-1519.
4. Adam F, Kauskot A, Rosa JP, Bryckaert M. Mitogen-activated protein kinases in hemostasis and thrombosis. *J Thromb Haemost*. 2008;6(12):2007-2016.
5. Korporaal SJA, Van Eck M, Adelmeijer J, et al. Platelet activation by oxidized low density lipoprotein is mediated by CD36 and scavenger receptor-A. *Arterioscler Thromb Vasc Biol*. 2007;27(11):2476-2483.
6. Shi P, Zhang L, Zhang M, et al. Platelet-specific p38α deficiency improved cardiac function after myocardial infarction in mice. *Arterioscler Thromb Vasc Biol*. 2017;37(12):e185-e196.
7. Adam F, Kauskot A, Nurden P, et al. Platelet JNK1 is involved in secretion and thrombus formation. *Blood*. 2010;115(20):4083-4092.
8. Yang M, Cooley BC, Li W, et al. Platelet CD36 promotes thrombosis by activating redox sensor ERK5 in hyperlipidemic conditions. *Blood*. 2017;129(21):2917-2927.
9. Chuang HC, Wang X, Tan TH. MAP4K family kinases in immunity and inflammation. *Adv Immunol*. 2016;129:277-314.
10. Meng Z, Moroishi T, Mottier-Pavie V, et al. MAP4K family kinases act in parallel to MST1/2 to activate LATS1/2 in the Hippo pathway. *Nat Commun*. 2015;6:8357.
11. Kaneko S, Chen X, Lu P, et al. Smad inhibition by the Ste20 kinase misshapen. *Proc Natl Acad Sci U S A*. 2011;108(27):11127-11132.
12. Yue M, Luo D, Yu S, et al. Misshapen/NIK-related kinase (MINK1) is involved in platelet function, hemostasis, and thrombus formation. *Blood*. 2016;127(7):927-937.
13. Jovanovic D, Yan S, Baumgartner M. The molecular basis of the dichotomous functionality of MAP4K4 in proliferation and cell motility control in cancer. *Front Oncol*. 2022;12:1059513.
14. Singh SK, Kumar S, Viswakarma N, et al. MAP4K4 promotes pancreatic tumorigenesis via phosphorylation and activation of mixed lineage kinase 3. *Oncogene*. 2021;40(43):6153-6165.
15. Nam GS, Kim S, Kwon YS, Kim MK, Nam KS. A new function for MAP4K4 inhibitors during platelet aggregation and platelet-mediated clot retraction. *Biochem Pharmacol*. 2021;188:114519.
16. Shitashige M, Satow R, Jigami T, et al. Traf2- and Nck-interacting kinase is essential for Wnt signaling and colorectal cancer growth. *Cancer Res*. 2010;70(12):5024-5033.
17. Larhammar M, Huntwork-Rodriguez S, Rudhard Y, Sengupta-Ghosh A, Lewcock JW. The Ste20 family kinases MAP4K4, MINK1, and TNIK converge to regulate stress-induced JNK signaling in neurons. *J Neurosci*. 2017;37(46):11074-11084.
18. Wu X, Zhang Z, Qiu Z, et al. TNIK in disease: from molecular insights to therapeutic prospects. *Apoptosis*. 2024;29(9-10):1361-1376.
19. Pham TCP, Dollet L, Ali MS, et al. TNIK is a conserved regulator of glucose and lipid metabolism in obesity. *Sci Adv*. 2023;9(32):eadf7119.
20. Dhungana H, Huuskonen MT, Jaronen M, et al. Sulfosuccinimidyl oleate sodium is neuroprotective and alleviates stroke-induced neuroinflammation. *J Neuroinflammation*. 2017;14(1):237.
21. Huang ZS, Zeng CL, Zhu LJ, Jiang L, Li N, Hu H. Salvianolic acid A inhibits platelet activation and arterial thrombosis via inhibition of phosphoinositide 3-kinase. *J Thromb Haemost*. 2010;8(6):1383-1393.
22. Li L, Zhou J, Wang S, et al. Critical role of peroxisome proliferator-activated receptor α in promoting platelet hyperreactivity and thrombosis under hyperlipidemia. *Haematologica*. 2022;107(6):1358-1373.
23. Whitmarsh AJ, Cavanagh J, Tournier C, Yasuda J, Davis RJ. A mammalian scaffold complex that selectively mediates MAP kinase activation. *Science (1979)*. 1998;281(5383):1671-1674.

24. Yarza R, Vela S, Solas M, Ramirez MJ. c-Jun N-terminal kinase (JNK) signaling as a therapeutic target for Alzheimer's disease. *Front Pharmacol*. 2015; 6:321.

25. Stebbins JL, De SK, Machleidt T, et al. Identification of a new JNK inhibitor targeting the JNK-JIP interaction site. *Proc Natl Acad Sci U S A*. 2008; 105(43):16809-16813.

26. Cameron SJ, Ture SK, Mickelsen D, et al. Platelet extracellular regulated protein kinase 5 is a redox switch and triggers maladaptive platelet responses and myocardial infarct expansion. *Circulation*. 2015;132(1):47-58.

27. Cheng Z, Gao W, Fan X, et al. Extracellular signal-regulated kinase 5 associates with casein kinase II to regulate GPIb-IX-mediated platelet activation via the PTEN/PI3K/Akt pathway. *J Thromb Haemost*. 2017;15(8):1679-1688.

28. Giardina JB, Tanner DJ, Khalil RA. Oxidized-LDL enhances coronary vasoconstriction by increasing the activity of protein kinase C isoforms α and ε. *Hypertension*. 2001;37(2 pt 2):561-568.

29. Raghuraman G, Zuniga MC, Yuan H, Zhou W. PKCε mediates resistin-induced NADPH oxidase activation and inflammation leading to smooth muscle cell dysfunction and intimal hyperplasia. *Atherosclerosis*. 2016;253:29-37.

30. Pears CJ, Thornber K, Auger JM, et al. Differential roles of the PKC novel isoforms, PKCδ and PKCε, in mouse and human platelets. *PLoS One*. 2008; 3(11):e3793.

31. Unsworth AJ, Finney BA, Navarro-Nunez L, Severin S, Watson SP, Pears CJ. Protein kinase Cε and protein kinase Cθ double-deficient mice have a bleeding diathesis. *J Thromb Haemost*. 2012;10(9):1887-1894.

32. Bynagari-Settipalli YS, Lakhani P, Jin J, et al. Protein kinase C isoform ε negatively regulates ADP-induced calcium mobilization and thromboxane generation in platelets. *Arterioscler Thromb Vasc Biol*. 2012;32(5):1211-1219.

33. Schürch C, Riether C, Matter MS, Tzankov A, Ochsenbein AF. CD27 signaling on chronic myelogenous leukemia stem cells activates Wnt target genes and promotes disease progression. *J Clin Invest*. 2012;122(2):624-638.

34. Chon HJ, Lee Y, Bae KJ, Byun BJ, Kim SA, Kim J. Traf2- and Nck-interacting kinase (TNIK) is involved in the anti-cancer mechanism of dovitinib in human multiple myeloma IM-9 cells. *Amino Acids*. 2016;48(7):1591-1599.

35. Ewald CY, Pulous FE, Lok SWY, et al. TNIK's emerging role in cancer, metabolism, and age-related diseases. *Trends Pharmacol Sci*. 2024;45(6): 478-489.